Available online at www.sciencedirect.com
SCIENCE DIRECT®
Catalysis Today 89 (2004) 363–368
CATALYSIS TODAY
www.elsevier.com/locate/cattod

Atomic and electronic structure dependence of surface chemical reactivity
The case of CO adsorption on a Pt/Co surface

Pierre Légaré [a,*], Gabriela F. Cabeza [b], Norberto J. Castellani [b]

[a] *Université Louis Pasteur, ECPM-LMSPC, 25 rue Becquerel, F-67087 Strasbourg, France*
[b] *Departamento de fisica, Universidad Nacional del Sur, Avenida Alem 1253, 8000 Bahia Blanca, Argentina*

Abstract

The chemical properties of Pt deposits on Co(0 0 0 1) in the range of Pt coverage up to 1.5 monolayer (ML) are presented. They are checked by CO adsorption at room temperature. We show that the CO total coverage decreases as the Pt coverage increases although both the (apparently) free Co areas as well as the Pt-covered areas do adsorb CO. This is a consequence of the CO/Pt adsorption energy lowering down to 0.8 eV as evaluated experimentally. This is interpreted in view of the observations performed by STM, LEED and photoemission on the Pt-covered surface, before and after CO exposure. Ab initio calculations performed on a Pt monolayer on Co(0 0 0 1) confirm the interpretation.

Keywords: Surface; Model catalysts; Experimental; Photoemission (XPS); STM; Theory; Co; Pt; CO

1. Introduction

During the past decade bimetallic surfaces, either metal overlayers or surface alloys, have been the subject of a tremendous activity [1]. This is because this kind of systems exhibit original physical as well as chemical properties due to their structural and electronic features. Thus, PtNi surface alloys have showed catalytic activities that do not resemble those of their pure components [2,3]. Ruban et al. [4] published a systematic study of the theoretical local electronic structure of pseudomorphic metal monolayers on various metallic substrates in connection with their chemical reactivity. They pointed out the importance of the d-band position on the adsorption properties. In a previous work, we studied the growth of Pt thin layers on Ni(1 1 1) [5] and Co(0 0 0 1) [6]. The growth of monoatomic-thick Pt islands on Co(0 0 0 1) was observed by scanning tunneling microscopy (STM) [6]. The adsorption properties of both systems were studied theoretically [7,8] and experimentally [9]. We showed that the adsorption energy of CO on the Pt islands grown on Co(0 0 0 1) was lower than on pure Pt(1 1 1) by about 40%. This was attributed to the compressive in-plane stress suffered by the islands.

In this paper, we present new results obtained for a larger Pt coverage range over Co(0 0 0 1), up to 1.5 monolayer, with or without thermal treatment of the deposits. The overlayer is characterized using STM and photoemission (XPS and UPS). Its chemical reactivity is checked by CO adsorption. To interpret the peculiarities of CO in interaction with this surface, we performed density functional theory (DFT)-based ab initio calculations. They rely on a slab model where a Co(0 0 0 1) substrate is capped with a Pt epitaxial (1 1 1) layer.

2. Experimental

The experiments were performed in a vessel comprising three interconnected high-vacuum chambers. The working pressure was in the low 10^{-9} mB range. The first chamber allows for low energy electron diffraction (LEED) observation of the sample surface. The central chamber is devoted to sample preparation and photoemission spectroscopy (XPS). It is equipped with a twin anode permitting the use of Al Kα and Mg Kα X-rays, and a hemispherical analyzer. A UV-lamp fed with He permitted the use of He I and He II

* Corresponding author. Tel.: +33-390-24-27-55; fax: +33-390-24-27-61.
E-mail address: legare@chimie.u-strasbg.fr (P. Légaré).

0920-5861/$ – see front matter © 2003 Elsevier B.V. All rights reserved.
doi:10.1016/j.cattod.2003.12.009

photons. Pt deposition from a resistively heated ribbon and CO exposures were also performed in this chamber. The third chamber permitted STM imaging of the sample with Pt–Ir tips. This was used to determine the overall surface morphology before and after Pt deposition. However, no atomic resolution could be obtained.

The sample was prepared by annealing and Ar-ions bombardment. The sample temperature was kept lower than 650 K in order to avoid the Co phase transition from hcp to fcc. C and O were the two contaminants detected at the surface. C could be entirely eliminated by the cleaning procedure. The residual O pollution was estimated to be lower than 5% of a monolayer. Pt was then deposited at room temperature at the approximate speed of 4×10^{-2} ML min^{-1}. In a first series of experiments, the sample was directly examined by STM and XPS or submitted to CO adsorption after Pt deposition ("as-deposited" results). In a second series of experiments, the freshly Pt-covered sample was first heated at 550 K for 2 h ("annealed" results). The Pt coverage θ(Pt) was estimated from the Pt 4f peaks recorded by XPS.

CO exposures were performed using the following procedure. CO was admitted to interact with the sample at a pressure of 3.6×10^{-7} mB at room temperature for 15 min. Then the pressure was decreased to 1.6×10^{-7} mB and the photoemission spectra were recorded. The aim of this procedure was to approach saturation of the surface during the first pressure step and then to obtain readily the equilibrium coverage in the second step, minimizing any possible evolution during the recording time. In order to reduce the working time of the X-ray source at this CO pressure, the spectra were generally recorded with a poor resolution (pass energy of 50 eV). A better resolution (pass energy of 20 eV) was however used in specific cases where overlapping components were to be separated.

3. Theoretical model

The ab initio calculations were performed with DACAPO [10] for total energy computation and electronic structure description. It is a program based on DFT using a plane wave basis set, in the generalized gradient approximation (GGA) with the Perdew–Wang functional (PW91) [11]. The electron–ion interactions are described by ultrasoft pseudopotentials [12]. The basis was limited by a high-energy cutoff at 450 eV. The Kohn–Sham one-electron equations were solved self-consistently. In order to take into account the magnetic properties of Co, the computations were conducted at the spin-polarized level. It was shown on Pt–Co multilayers, that Pt couples magnetically at the Co interface [13]. It can be important to take this effect into account for a good description of the Pt chemical behavior.

Our model consisted of a four-layer slab formed by three Co(0 0 0 1) planes and one pseudomorphic Pt plane in the hcp stacking sequence. CO was adsorbed in the on-top geometry on the Pt side with a 1/3 ML coverage so that the periodic surface mesh was $(\sqrt{3} \times \sqrt{3})R30^\circ$ as observed experimentally. The slab was repeated periodically in the direction perpendicular to the (0 0 0 1) surface with vacuum spacing between the periodic images of at least 12 Å. The equilibrium parameters of bulk hcp Co given by our method were $a = 2.503$ Å and $c = 4.044$ Å. During the calculations, the first Brillouin zone was sampled using a $(6 \times 6 \times 1)$ Monkhorst-Pack grid for the CO-covered slab or a $(10 \times 10 \times 1)$ grid for the (1×1) uncovered slab.

The adsorption energy is calculated as the energy difference between the CO-covered slab and the fragments (free CO molecule and uncovered slab). The sign was changed in order to obtain positive adsorption energy as usual.

We note that a previous study using a similar method showed that our Pt/Co model is stable and permitted evaluation of the Pt layer adhesion on Co(0 0 0 1) [14]. The adsorption of CO on metals with various DFT-based codes is now common in the literature [15]. Although this technique showed some limitations to discriminate adsorption sites of close adsorption powers [15,16], it gives reasonable evaluation of adsorption energies and bond description.

4. Results and discussion

The freshly prepared surface was examined with STM before and after Pt deposition. Fig. 1 gives some examples of the as-deposited (Pt coverage 0.12 ML) and annealed (Pt coverage 0.18 ML) surface. We can recognize the same features among the four images. Dendritic Pt islands appear on the Co terraces. Cross-section measurements show that they are 1 ML thick, with apparent thickness ranging from 2.3 to 2.5 Å [6]. The clean Co(0 0 0 1) surface was also examined using STM. The surface exhibited flat terraces several hundred angstroms wide, separated by monoatomic or sometimes diatomic steps [6]. These steps were more or less linear at a scale length of ca. 500 Å. On the contrary, the images reported in Fig. 1 show dendritic shapes along the step edges, similar to the island edges. Obviously, the step edges were modified by Pt deposition. Actually, most of the Pt atoms deposited on a terrace diffuse to the ascending step where they could nucleate and only a limited fraction of them nucleate on the terraces to form the islands. Examination of the various pictures of Fig. 1 does not permit to discriminate between the as-deposited and the annealed samples. This proves that, at the scale permitted with our STM pictures, no drastic rearrangement happens under mild heating conditions. We interpret this dendritic shape of the Pt islands as an indication of the strain induced by the misfit between the overlayer and the Co substrate. Highest Pt coverages make the islands grow wider and wider. However, no perfect Pt monolayer could be obtained as a second Pt layer starts growing beyond a deposited quantity in the 0.5 ML range. We refer to a previous paper [6] for a more detailed account of the STM observations on the as-deposited samples. It is worth noting now that

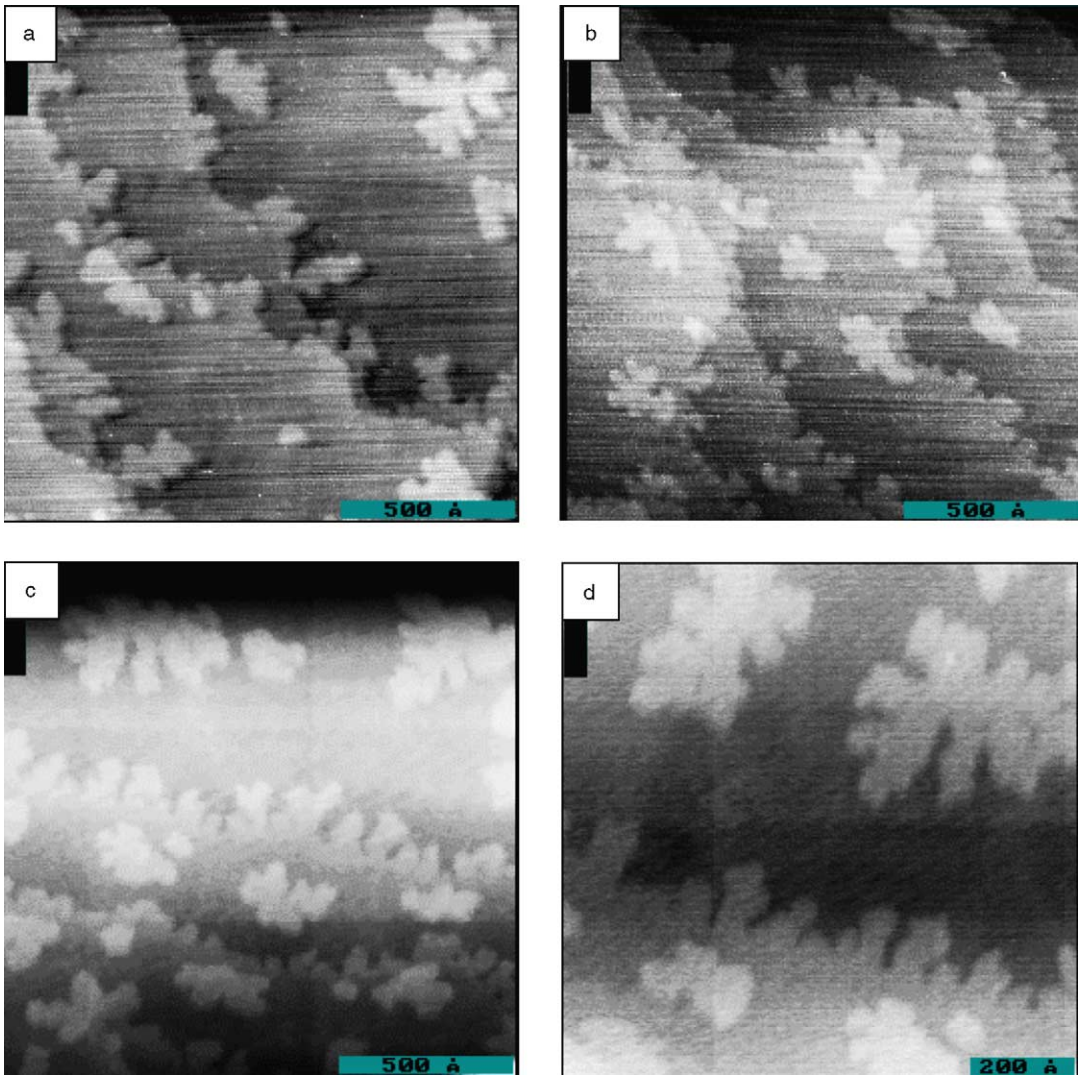

Fig. 1. STM pictures of the Co(0 0 0 1) surface after Pt deposition. (a) and (b) as-deposited, θ(Pt) = 0.12 ML, 150 nm × 150 nm; (c) annealed sample, θ(Pt) = 0.18 ML, 150 nm × 150 nm; (d) annealed sample, θ(Pt) = 0.18 ML, 100 nm × 100 nm.

LEED observations showed that the (1 × 1) picture was apparently unaffected by Pt deposition. This and the STM pictures suggest that the Pt layer grows in registry with the Co surface, at least at coverages lower than one monolayer.

Using XPS the Pt 4f peaks were recorded before and after the annealing treatment. They could not be discriminated by a simple observation of the binding energy (71.05 eV for the Pt $4f_{7/2}$ peak) and intensity. However, we note that this binding energy indicates an upward shift by 0.4 eV when compared to the pure surface Pt 4f peaks binding energy [17]. Moreover, the difference between the two spectra (annealed minus as-deposited) exhibit a faint residue shifted by 0.4 eV to high binding energies with respect to the peaks maxima. This could be compared with a Pt component located at 71.40 eV attributed to Pt diluted in the first layers of Co by Bulou et al. [18]. This could suggest that Pt started to diffuse in the Co surface during the annealing treatment.

We now report in Fig. 2 the intensity change of the O 1s signal recorded by XPS after CO exposure versus the Pt

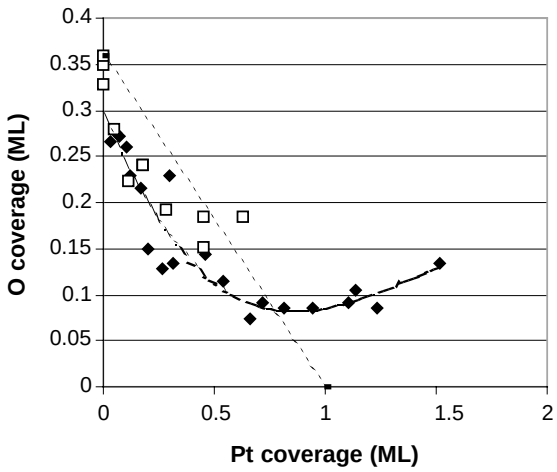

Fig. 2. Evolution of the O 1s intensity after CO exposure vs. Pt coverage. Empty squares: as-deposited Pt; filled diamonds: annealed sample. The curve is a guide for the eyes. Broken line: see text.

coverage. This gives two series of data depending on the Pt treatment before exposure. We note that LEED observation of pure Co(0 0 0 1) during CO exposure shows the formation of a $(\sqrt{3} \times \sqrt{3})R30^\circ$ pattern superimposed to a $(\sqrt{7/3} \times \sqrt{7/3})R10.9^\circ$ pattern as already reported by various authors [19,20]. These structures were attributed a CO coverage of 0.3 and 0.43 ML, respectively. Our own calibration [9] gives 0.36 ML for the highest CO coverage we could obtain in this study. We think this is in perfect agreement with Ref. [19] as the $(\sqrt{7/3} \times \sqrt{7/3})R10.9^\circ$ pattern did not cover the entire surface area. The most striking feature appearing in the figure is the rapid decrease of the adsorbed CO coverage as soon as some Pt is deposited on the surface. Then, beyond a Pt coverage of 0.5 ML, the signal tends to stabilize around a mean CO coverage of 0.18 and 0.1 ML for the as-deposited and annealed data, respectively. Moreover, this decrease is specially pronounced for the annealed samples. The simpler hypothesis to interpret this would be to consider that CO can only adsorb on the fractional area unoccupied by Pt on the surface. We have drawn in Fig. 2 (broken line) the evolution expected for the O 1s intensity under this assumption. The experimental data are clearly lower up to a Pt coverage of 0.5 ML.

Actually, we already presented evidence [9] that CO adsorbs on the Pt islands. A comparison of the Pt 4f peaks by XPS before and after CO exposure shows that the two peaks of the doublet are split into two components by CO: one is similar to the corresponding clean signal whereas the other one is shifted to higher binding energies by 0.8 eV. The intensity ratio between the shifted and unshifted signals showed that the CO coverage on Pt was 1/3 ML at low Pt coverage but decrease more or less linearly when the Pt coverage increases. This permitted also to separate the O 1s signal into two components. The signal corresponding to CO adsorbed on the Co areas appeared at 531.8 eV whereas that corresponding to CO adsorbed on Pt was at 532.6 eV. A comparison with Ref. [9] showed that this could be attributed to CO adsorbed in the on-top geometry on both metals.

Finally, all these results show that, for the same equilibrium pressure, the CO coverage decreases on both metals as the Pt coverage increases showing that the surface properties of both metals are modified. On Co, this could be due to the diffusion of some Pt atoms in the Co surface plane. This is suggested by our experimental results following the annealing treatment. We suppose that this could already take place, although at a lower extent, for the unannealed sample. In the case of the Pt islands, we believe that the following results obtained by the ab initio calculations present evidences on the origin of this chemical reactivity change.

We first searched for the equilibrium clean surface of our slab model by relaxing the Pt layer and the Co layer at the interface. This gives a Co–Pt interplane distance of 2.287 Å. The first Co–Co interplane distance was only slightly decreased when compared to that of the theoretical Co-bulk (2.000 Å compared to 2.022 Å). We present in Fig. 3a the density of states projected on the Pt atom. It can be compared

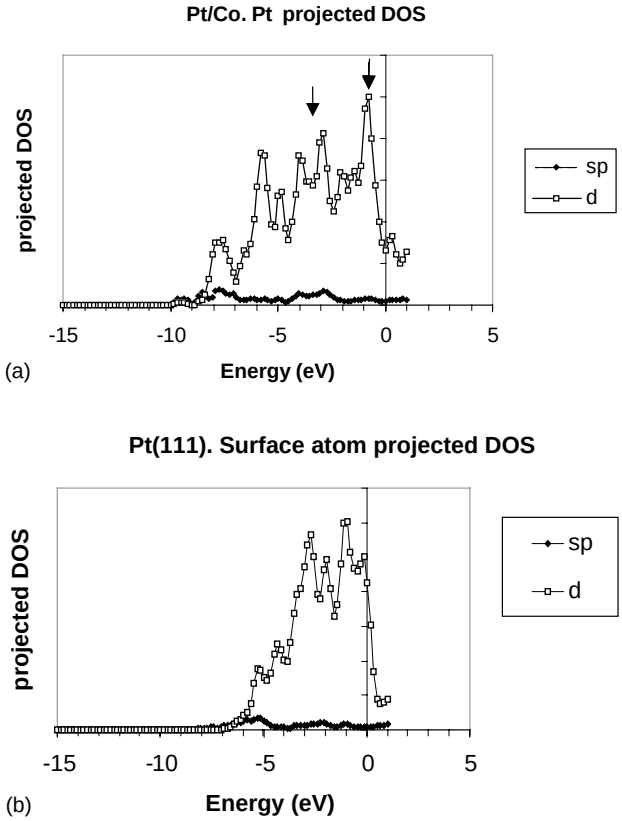

Fig. 3. (a) Pt projected density of states of the clean (CO uncovered) Pt–Co slab. (b) Projected density of state on the surface atom of a four-layer Pt slab. The origin of the energy scale corresponds to the Fermi level.

to the projected density of states on the Pt surface atom of a four-layer Pt slab reported in Fig. 3b. A first striking feature of Fig. 3a is the extension of the Pt d-band down to −8 eV whereas it does not extend below −6 eV in Fig. 3b. Actually, the center of gravity of the d-states is around −3.26 eV for Pt/Co and −2.11 eV for the pure Pt surface. This valence band broadening is mainly due to the Pt–Pt distance reduction from pure Pt to Pt/Co. Moreover, the Fermi level corresponds to a region of low density of states in Fig. 3a and high density in Fig. 3b. This permits a first comparison with our experimental results. The analysis of the Pt 4f peaks obtained by XPS for the freshly Pt-covered Co surface showed that its asymmetry parameter was clearly decreased with respect to that of the clean Pt(1 1 1) surface [6]. This is a clear indication of the low density of states at the Fermi level at the Pt site of the Pt/Co surface [21,22]. We also note that dominant features appear in the Pt d-band reported in Fig. 3a around −1 and −4 eV below the Fermi level as indicated by arrows. Fig. 4 reproduce the UV-excited photoemission spectra (UPS) recorded after deposition of Pt on Co(0 0 0 1) at various coverages. The arrows indicate the main Pt-induced features in good agreement with the theoretical results. It is thus obvious that our model captures the essential electronic properties of the real Pt/Co surface. It is principally characterized by the short Pt–Pt distances (2.53 Å) corresponding

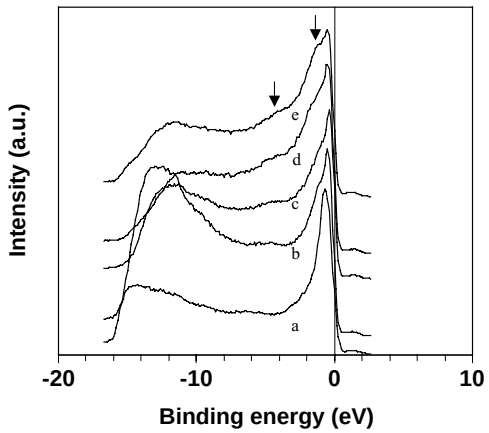

Fig. 4. UPS (He I) curves for various Pt deposits: (a) clean Co(0 0 0 1) surface; (b) θ(Pt) = 0.1 ML; (c) θ(Pt) = 0.2 ML; (d) θ(Pt) = 0.3 ML; (e) θ(Pt) = 0.5 ML.

to the in-plane Co–Co distance. Its electronic properties are a direct consequence of this special geometry.

We now look at the chemical behavior of the Pt overlayer as it could be described by our model. The total energies of the CO-covered slab (with freely relaxed Pt–C and C–O distances) and the separated fragments were computed. The resulting adsorption energy was 0.53 eV, with Pt–C and C–O distance of 1.965 and 1.166 Å, respectively. This adsorption energy should be compared to a theoretical value of 1.45 eV for the clean Pt(1 1 1) surface [23]. The drastic lowering of the CO adsorption energy given by our model is nothing but the consequence of the high Pt–Pt distance reduction as proved by an ab initio study of CO and O adsorption on Ru in dependence with the Ru surface parameter [24]. Following Hammer and Norskov [25], this could be expected from the downward shift of the d-band center as reported above, the effect of which is to decrease the coupling between the Pt d-states and the CO 2π states. We note that this is also in good qualitative agreement with the CO adsorption energy (0.8 eV) that we obtained by analysis of the CO-induced binding energy shift of the Pt 4f photoemission peaks on Pt/Co [9], the same method giving 1.3 eV for CO on the pure Pt(1 1 1) surface.

The fact that our static model of CO adsorption on Pt/Co gives good agreement with our experimental results suggests that it capture the essential features of the real Pt deposits in our experimental conditions, and that no important surface restructuring is induced by CO adsorption. This is in contrast to Pt(1 0 0) where CO induces a lifting of the hexagonal reconstruction to the square (1 × 1) configuration. We note that the reconstructed Pt(1 0 0) surface has some 20% atomic density in excess of the (1 × 1) surface, and could in this sense present some similarity with our Pt/Co surface. The mechanisms of the CO-induced deconstruction of Pt(1 0 0) was studied by van Beurden et al. [26] using molecular dynamics (MD) simulations with DFT-based parameterized potentials. This unable the authors to use a model with 1800 surface Pt atoms and to take the temperature into account. This is largely beyond the possibility of pure DFT calculations as we used. It would be however desirable to apply MD simulations to our system, for example to know the limits of its stability and to make clear its possible evolution under reactive conditions.

5. Conclusion

We presented an account of the chemical properties of Pt islands supported on Co(0 0 0 1) as checked by CO adsorption. The surface was first characterized by STM, LEED, XPS and UPS. STM and LEED suggested that the Pt overlayer could grow pseudomorphically with the Co substrate in the investigated range of Pt coverage. Upon CO exposure at room temperature, the equilibrium CO coverage decreased as the Pt coverage increased. However, the analysis showed that both the Co as well as the Pt areas could adsorb CO. The experimental results indicate that both metals had modified chemical properties. On the Co areas, this could be the consequence of some Pt dilution in the first layer. On Pt, this low affinity toward CO was attributed to the Pt in-plane compression. This interpretation was supported by ab initio calculations using a model of a Pt overlayer on Co which reproduced the main electronic and chemical experimental observations.

Acknowledgements

The computations have been performed with the help of the Centre Universitaire Régional de Ressources Informatiques (CURRI) and the Centre Informatique National de l'Enseignement Supérieur (CINES).

References

[1] J.A. Rodriguez, Surf. Sci. Rep. 24 (1996) 223.
[2] S. Aeiyach, F. Garin, L. Hilaire, P. Légaré, G. Maire, J. Mol. Catal. 25 (1984) 183.
[3] J.C. Bertolini, B. Tardy, M. Abon, J. Billy, P. Delichère, J. Massardier, Surf. Sci. 135 (1983) 117.
[4] A. Ruban, B. Hammer, P. Stoltze, H.L. Skriver, J.K. Norskov, J. Mol. Catal. A 115 (1997) 421.
[5] M. Romeo, J. Majerus, P. Légaré, N.J. Castellani, D.B. Leroy, Surf. Sci. 238 (1990) 163.
[6] G.F. Cabeza, P. Légaré, A. Sadki, N.J. Castellani, Surf. Sci. 457 (2000) 121.
[7] G.F. Cabeza, N.J. Castellani, P. Légaré, Surf. Rev. Lett. 6 (1999) 369.
[8] G.F. Cabeza, N.J. Castellani, P. Légaré, Comp. Mater. Sci. 17 (2000) 255.
[9] G.F. Cabeza, P. Légaré, N.J. Castellani, Surf. Sci. 465 (2000) 286.
[10] (a) B. Hammer, L.B. Hansen, J.K. Norskov, Phys. Rev. B 59 (1999) 7413;
(b) http://fysik.dtu.dk/CAMPOS.
[11] J.P. Perdew, J.A. Chevary, S.H. Vosko, K.A. Jackson, M.R. Pederson, D.J. Singh, C. Fiolhais, Phys. Rev. B 46 (1992) 6671.
[12] J.P. Vanderbilt, Phys. Rev. B 41 (1990) 7892.

[13] C. Ederer, M. Komelj, M. Fähnle, G. Schütz, Phys. Rev. B 66 (2002) 094413.
[14] P. Légaré, N.J. Castellani, G.F. Cabeza, Surf. Sci. 496 (2002) L51.
[15] P.J. Feibelman, B. Hammer, J.K. Norskov, F. Wagner, M. Scheffler, R. Stumpf, R. Watwe, J. Dumesic, J. Phys. Chem. B 105 (2001) 4018.
[16] I. Grinberg, Y. Yourdshahyan, A.M. Rappe, J. Chem. Phys. 117 (2002) 2264.
[17] P. Légaré, G. Lindauer, L. Hilaire, G. Maire, J.-J. Ehrhardt, J. Jupille, A. Cassuto, C. Guillot, J. Lecante, Surf. Sci. 198 (1988) 69.
[18] H. Bulou, A. Barbier, R. Belkou, C. Guillot, B. Carrière, J.P. Deville, Surf. Sci. 352 (1996) 828.
[19] H. Papp, Surf. Sci. 129 (1983) 205.
[20] J. Lahtinen, J. Vaari, K. Kauraala, Surf. Sci. 418 (1998) 502.
[21] S. Doniach, M. Sunjic, J. Phys. C 3 (1970) 285.
[22] W.F. Egelhoff, Surf. Sci. Rep. 6 (1987) 253.
[23] B. Hammer, Y. Morikawa, J.K. Norskov, Phys. Rev. Lett. 76 (1996) 2141.
[24] M. Mavrikakis, B. Hammer, J.K. Norskov, Phys. Rev. Lett. 81 (1998) 2819.
[25] B. Hammer, J.K. Norskov, Catal. Lett. 46 (1997) 31.
[26] P. van Beurden, B.S. Bunnik, G.J. Kramer, A. Borg, Phys. Rev. Lett. 90 (2003) 066106.